Interseismic fault strengthening and earthquake-slip instability: Friction or cohesion?

Sankar K. Muhuri*
Thomas A. Dewers
School of Geology and Geophysics, University of Oklahoma, Norman, Oklahoma 73019, USA
Thurman E. Scott Jr. Poromechanics Institute, University of Oklahoma, Norman, Oklahoma 73019, USA
Ze'ev Reches Institute of Earth Sciences, Hebrew University, Jerusalem 91904, Israel

ABSTRACT

The slip instability of an earthquake and its abrupt energy release depend primarily on the intensity of strength drop during accelerated fault slip. This process is typically attributed to changes of frictional resistance between two sliding blocks. Here we show that friction changes alone cannot explain observed strength variations of artificial fault zones. Sandstone samples with saw-cut faults and gypsum gouge zones were subjected to many cycles of hold-slide loading. Samples with water-saturated gouge display (1) systematic, time-dependent increase of gouge strength; (2) unstable failure of gouge with large stress drops; and (3) lithification of gouge by crack sealing, recrystallization, porosity reduction, and grain bonding. All these features are absent in identical tests with dry gouge. These observations indicate that gouge particles are cemented by chemical processes during hold periods and suggest that the cyclical strength variations are controlled by cohesion strengthening rather than by friction changes. We further hypothesize that crustal fault zones could be lithified during the interseismic stage, and this lithification would control earthquake-slip instability.

Keywords: earthquakes, fault strengthening, friction, cohesion, slip instability.

INTRODUCTION

Earthquake processes need to be understood on multiple time scales: slip instability, rupture, and ground motion operate on seconds to minutes, whereas healing and restrengthening are active from days to centuries of the interseismic period (National Research Council, 2002). The slip instability is controlled by a complex combination of mechanical and chemical processes along an active fault. The dominant mechanical processes are growth and wear of asperities, grain crushing, and grain rotation (Dieterich and Kilgore, 1994; Marone and Scholz, 1989; Mair and Marone, 1999; Byerlee et al., 1978; Power et al., 1988). The chemical processes include cementation, recrystallization, grain bonding, pressure solution, and crack sealing (Sleep and Blanpied, 1992; Olsen et al., 1998). Chemical activity over a long time could strengthen fault gouge, and this strengthening would determine earthquake recurrence and severity: for slip to occur, fault shear stresses should exceed strength gained by such chemical activity.

To investigate these effects, we conducted month-long experiments with cyclical loading of laboratory fault zones. The sample geometry consisted of cylindrical precut sandstone blocks with an intervening fault zone similar to those used for investigation of frictional sliding over shorter durations (Byerlee et al., 1978; Olsen et al., 1998; Karner et al., 1997). The gypsum gouge within fault zones was either water saturated or nominally dry, and the experiments include as many as 15 hold-slide cycles for a single sample. We used gypsum gouge because of its fast reaction rates in water at room temperature. Further, it is shown that strengthening of gypsum gouge at room temperature is similar to strengthening of quartz gouge at elevated temperature. We thus argue that the present experiments capture aspects of gouge behavior under conditions of mid-crustal seismogenic depth, and that the experimental behavior is phenomenologically similar to earthquakes along crustal faults.

EXPERIMENTAL METHODS

The experiments were conducted using cylinders of Berea Sandstone, 25 mm in diameter and 60 mm in length, with a surface-ground precut at 30° to the sample long axis. The sandstone porosity (~20%) and permeability (~100 mD) facilitate gouge sandstone pore-pressure equilibration during the experiments. The 4-mm-thick gouge layer in each experiment was composed of natural gypsum sand (White Sands National Monument, New Mexico, United States) with a mean particle size of 125 μm. Distilled water was used as pore fluid in wet experiments. Experiments were run at room temperature in a triaxial cell under confining pressure of 20.7 MPa and pore pressures of 6.9 MPa. The experiments include multiple cycles of loading, up to 15 hold-slide cycles for a single sample, up to six orders of magnitude of hold periods (10 to 10^6 s), and axial strain rates of 2.6×10^{-5} s^{-1} for sliding cycles. Each experiment began with a hydrostatic hold period, with subsequent hold periods under axial (shear) loading. In a slide stage, samples were axially shortened at constant confining pressure to a predetermined strain. During hold periods, confining pressure and pore pressure were held constant, while axial stress was allowed to relax. The shear and normal stresses on the experimental fault were calculated using the effective axial and confining loads. The resulting pore volume loss was monitored with a volumometer with resolution of 0.0047 cm^3. Three experiments were run with water-saturated samples and one with a nominally dry sample.

EXPERIMENTAL RESULTS

The ratio τ/σ_n of shear and normal stresses acting on an experimental fault is plotted with respect to fault-parallel displacement in Figure 1A. This plot is for an experiment with 15 hold-slide cycles that was conducted in the presence of pore water. The hold periods were increased in order-of-magnitude steps from 10 s to 10^6 s (~12 days), and then decreased in steps to 10 s. The sample was preloaded hydrostatically under a mean effective stress of 13.9 MPa and then axially loaded until sliding was initiated. The initial hydrostatic loading produced a nonlinear stress-strain curve reflecting compaction of unconsolidated gouge.

Each of the cycles in Figure 1A displayed a series of characteristic stages. First, τ/σ_n increased linearly, reflecting elastic loading; the slope of this increase in stress-strain space is ~14.5 GPa, which approximates the weighted Young's modulus of Berea Sandstone with 4-mm-thick gypsum gouge. Second, the stress ratio τ/σ_n increased up to a peak strength (P in Fig. 1A, inset) followed by a stress drop. Although not shown here, the stress drop was accompanied by appreciable dilation in the gouge zone (Muhuri, 2002). Third, the stress ratio τ/σ_n attained a nearly constant sliding strength (S in Fig. 1A, inset) during a period of stable sliding. Fourth, after axial shortening was halted, the stress ratio τ/σ_n was relaxed by spontaneous creep.

*Present address: ChevronTexaco Exploration and Production Technology Company, Bellaire, Texas 77401, USA.

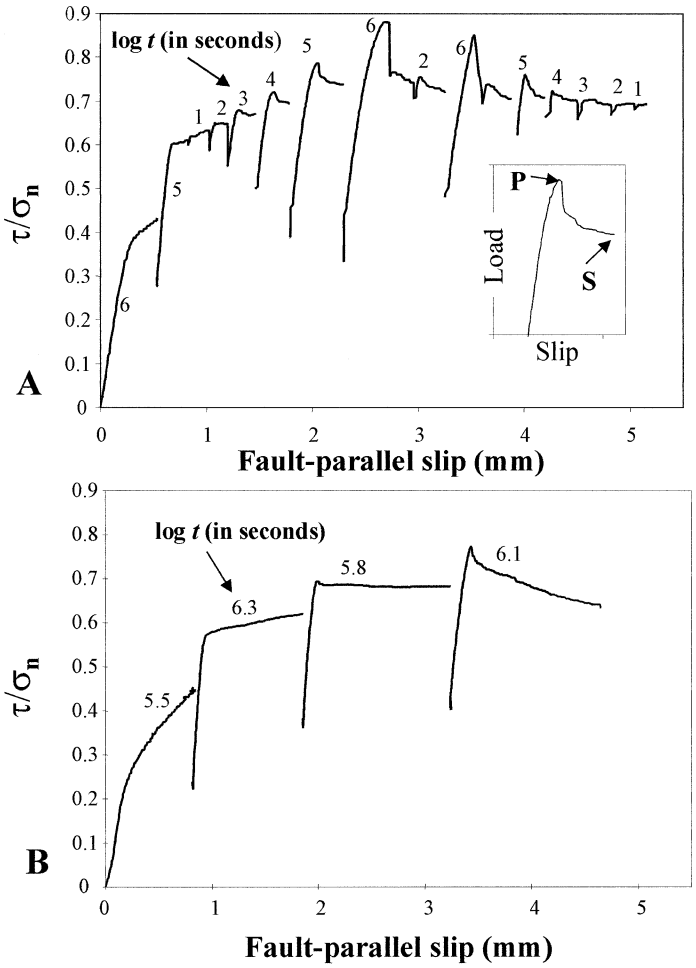

Figure 1. Loading history of hold-slide testing of sandstone samples with artificial fault (saw-cut) filled with gypsum gouge and deformed at room temperature. Sample is 25 mm diameter by 60 mm long, with principal stress directions and saw-cut oriented at 30° to vertical loading axis. Apparent friction coefficient [shear stress divided by normal stress (τ/σ_n)] on fault plane is plotted against cumulative fault-parallel displacement. Duration of each hold period that precedes each sliding event is marked by log *t*, where *t* is holding time. A: Results of water-saturated sample with 15 hold-slide cycles. Note that strengthening is proportional to hold time and clear stress drop after failure. B: Results for dry sample with four hold-slide cycles. Note buildup of stress followed by stable sliding along gouge zone and absence of marked peak strength shown in A.

One experiment (Fig. 1B) was run with a nominally dry sample subjected to the same effective loading conditions as in the previous tests. After an initial compaction phase, the gouge was subjected to four hold-slide cycles with hold periods of 10^5–10^6 s. Following the initiation of sliding, τ/σ_n remained at a quasi-constant value that reflects stable sliding along the fault zone. Similar behavior was observed in previous precut experiments over shorter durations (Logan et al., 1992). The peak strengths and subsequent stress drops that dominate water-saturated tests with long hold times (Fig. 1A) are apparently absent in tests run with nominally dry gouge (Fig. 1B). We attribute this difference to chemical processes that could be active only in water-saturated tests, in contrast to mechanical processes that were active in both wet and dry tests (see subsequent discussion).

ANALYSIS

The stress ratio τ/σ_n curve in Figure 1A reveals that the intensities of peak strengths and stress drops increase with holding duration. We analyze this strengthening of gouge in terms of the Coulomb failure criterion: $\tau = C + \mu\sigma_n$, where C is the cohesion (that does not depend on normal stress) and μ is the coefficient of internal friction. The Coulomb criterion was also used to evaluate the friction between two sliding blocks, best known as Byerlee's Law, $\tau = \mu_f\sigma_n$, where μ_f is the coefficient of friction.

The cohesion reflects the strength of the bonds between rock particles. Thus, the cohesion value is the combined magnitude of shear strength and normal strength of the bonding between grains. Friction, on the other hand, reflects the strength of asperities that resist slip between sliding blocks (Jaeger and Cook, 1979, p. 54). Thus, the friction coefficient is approximately the ratio between shear strength and normal strength of asperities. As this ratio (shear strength/normal strength) is fairly constant for most rocks, the friction coefficient is also fairly constant: for bare rock surfaces $\mu_f \sim 0.85$ (under $\sigma_n < 120$ MPa) and $\mu_f \sim 0.6$ (under $\sigma_n > 120$ MPa); for powdered gouge, μ_f ranges from 0.6 to 0.8 with typical values of 0.60–0.65.

We now examine one central question: Does gouge strengthening reflect frictional processes (strengthening of asperities) or does it represent a gain in cohesion (strengthening of bonded contacts between grains)? We define here two end-member models: frictional strengthening, manifested by an increase of friction coefficient μ_f while assuming no cohesive strength, and cohesion strengthening, manifested by an increase in cohesion C while assuming constant friction coefficient. Because our experiments were conducted under constant confining pressure, one cannot distinguish uniquely between these end members. To evaluate the relative dominance of each, we compare each model to known rock mechanics data (Fig. 2).

For frictional strengthening, we plotted the peak strength values of the friction coefficient, $\mu_f = \tau/\sigma_n$, as a function of holding time *t* for the wet test of Figure 1A (solid triangles in Fig. 2A). Also plotted are the sliding strength values of the same experiment (solid squares), as well as the peak strength values (open triangles) and sliding strength values (open squares) of the dry experiment of Figure 1B. The peak strength values for the wet experiment increase from $\mu_f \sim 0.61$ initially to $\mu_f \sim 0.87$ after 10^6 s. The sliding strength values appear to saturate at $\mu_f \sim 0.72$ after $\sim 10^5$ s. This increase of friction coefficient from 0.61 to 0.87 is large and in sharp contrast to Byerlee's Law. Note that only one material was used here and the normal stress varied modestly. For cohesion strengthening, we substituted the experimental measurements into the Coulomb criterion $C = \tau - \mu\sigma_n$. In these calculations, plotted in Figure 2B for the same data points of Figure 2A, the initial cohesion of gouge is taken as zero and $\mu = 0.61$ does not change with hold time (μ equal to 0.61 was measured in cycles with no holding in our experiments). The calculated cohesion for the peak strength increases monotonically with hold time to almost 8.0 MPa at 10^6 s; this increase fits a relation of $C = 0.48 \ln(t) - 0.95$ ($R^2 = 0.85$), where C is given in MPa and hold time *t* in seconds. Figure 2 strongly suggests that the observed strengthening could not be primarily frictional because one would not expect such a large increase in friction coefficient. The results thus indicate dominance of cohesion strengthening with modest increase in cohesion. This interpretation is further supported by widespread evidence of gouge cementation, as described in the next paragraph.

The microstructural observations and scanning electron microscope photomicrographs of wet gouge deformed at long hold times (Fig. 3A) show that grain boundaries are barely conspicuous, the porosity is totally obliterated, and the grains are bonded together (wb in Fig. 3A). Further, the wet gouge exhibits trails of fluid inclusions resulting from healing of microfractures (hf in Fig. 3A). This behavior presumably results from a combination of grain-boundary migration, stress- or strain-induced solution mass transfer (c in Fig. 3A), plastic flow, and grain interpenetration. This distinct texture of the wet samples is in contrast to remnant intergranular porosity in deformed dry

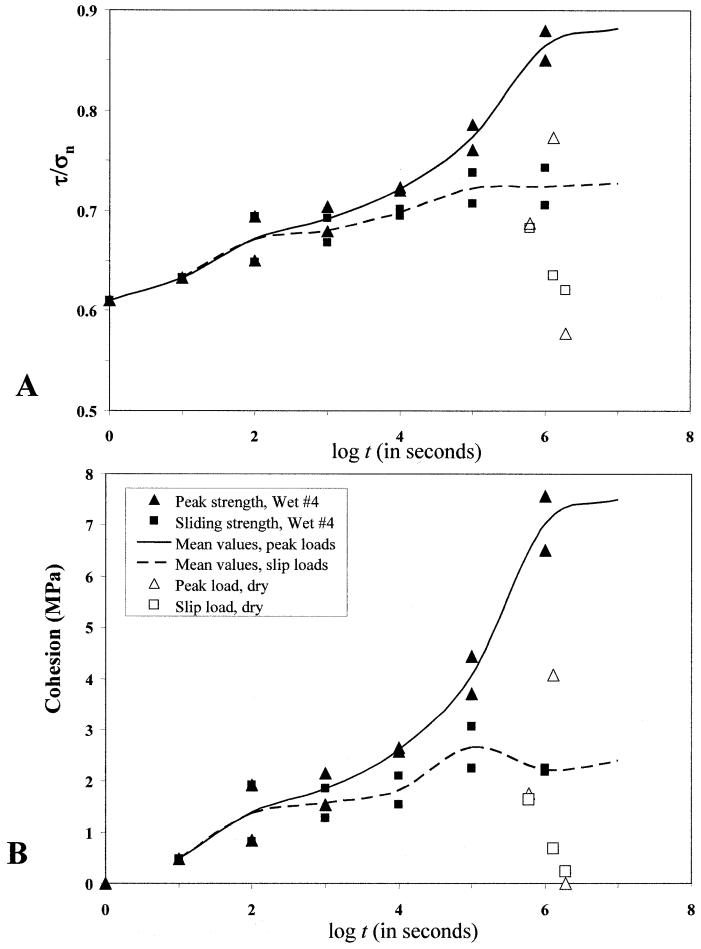

Figure 2. Strength variations of gypsum gouge as function of hold time; data from Figure 1. A: Strength is plotted as apparent friction coefficient (τ/σ_n) on fault by assuming vanishing cohesion. B: Strength is plotted by assuming cohesion increase and constant friction coefficient of 0.61. Solid triangles and solid squares—peak strength and slip strength, respectively, in water-saturated test of Figure 1A; open triangles and open squares—equivalent values for dry sample (Fig. 1B). Note that frictional strengthening (in A) requires friction coefficient increase from ~0.6 to ~0.9.

gouge (dark areas denoted p in Fig. 3B), as well as the extensive microfracturing and cataclasis and intracrystalline plastic deformation. Further, rounded grain boundaries (marked g in Fig. 3B) and open microfractures (f in Fig. 3B) in dry gouge are absent in the water-saturated, long-hold-time experiments.

In summary, while we cannot distinguish uniquely between friction strengthening and cohesion strengthening, the evaluation of macroscopic stress relations as well as the microstructural observations suggest dominance of the second mechanism. The following discussion suggests that cohesion strengthening can be recognized in other experiments and in the field.

DISCUSSION

The mechanical data (Figs. 1A and 2) and microstructural observations (Fig. 3) demonstrate that lithification effectively strengthens fault gouge. This behavior is not limited to gypsum. Karner et al. (1997) conducted strengthening experiments by using a saw-cut configuration similar to the present one with quartz gouge. To shorten the strengthening time of quartz gouge, the samples were held at 636 °C for periods up to one day, the temperature was lowered to 230 °C, and then loaded to failure at this temperature. Figure 4 displays the strengthening of gypsum gouge in the present experiments (solid dia-

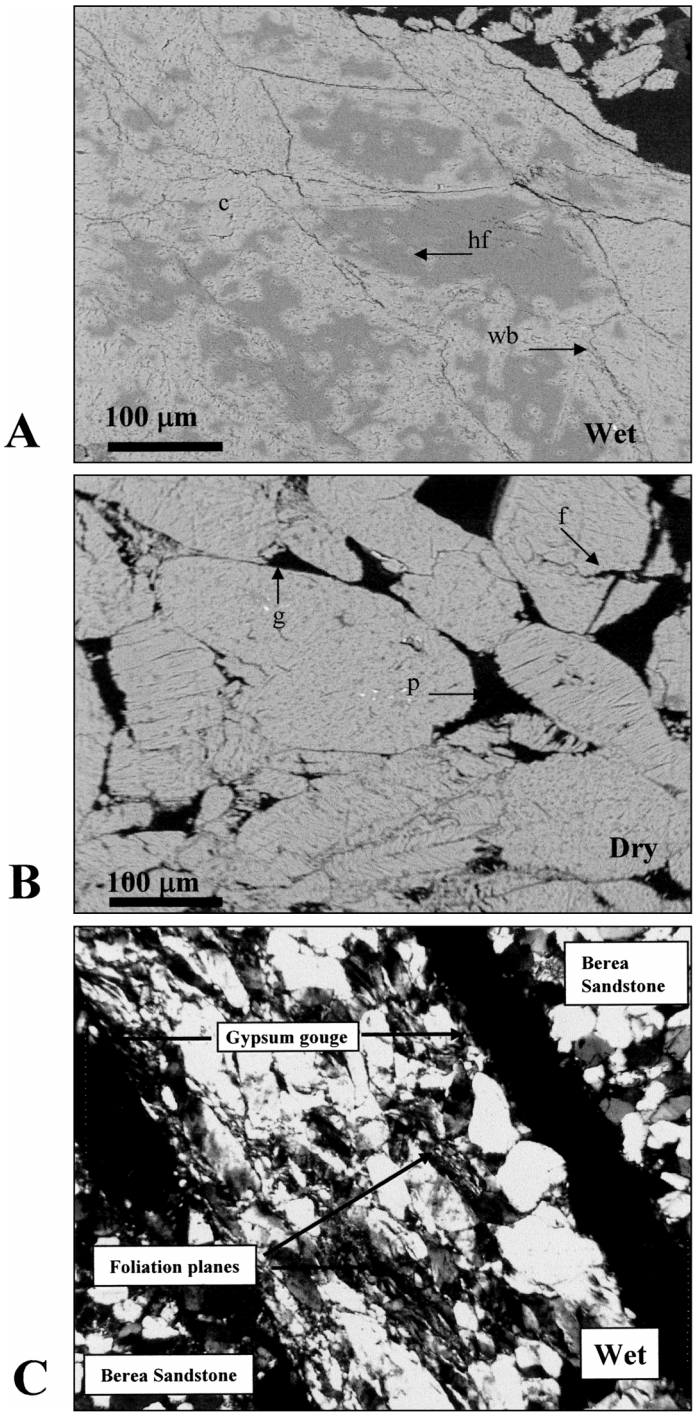

Figure 3. Backscattered scanning electron microscope (SEM) photomicrographs showing texture of experimentally deformed gouge. A: Wet gouge shows bonded grains that obscure original boundaries (wb), healed microfractures revealed by fluid-inclusion trails (hf), and recrystallization (c). B: Dry gouge shows distinct grain boundary (g), intergranular pore space (p), and abundant open microfractures (f); note absence of these features in wet gouge. Deformation conditions were similar in both cases (effective pressure of 13.8 MPa, ~60 days, and 7% axial shortening). C: Optical photomicrograph of water-saturated gouge zone under crossed polarizers; note uncrushed grains and foliated shear surfaces. Gypsum has separated from Berea Sandstone blocks during thin-section preparation process.

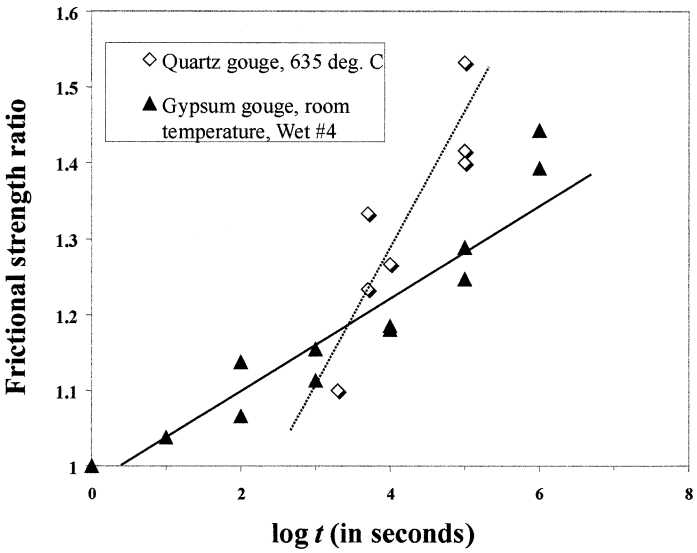

Figure 4. Gouge strengthening plotted as ratio of apparent friction coefficients: $(\tau/\sigma_n)_{initial}/(\tau/\sigma_n)_{final}$ at marked holding time. Gypsum gouge (this study, solid triangles with regression line: strength ratio = 0.064 × ln t + 0.977, where t = time; r^2 = .76) and quartz gouge (after Karner et al. [1997]; open diamonds with regression line: strength ratio = 0.170 × ln t + 0.603; r^2 = .79). Gypsum held and sheared at room temperature; quartz held at 635 °C and sheared at 230 °C (see text).

monds) compared to strengthening of quartz gouge (solid squares) in Karner et al. (1997). For sake of comparison, the measured peak strength (τ/σ_n) after holding is normalized by the same parameter for samples at zero hold time. The two types of gouge display a similar mode of time dependence, while the quartz gouge strengthens at a higher rate due to the high temperature during holding. The dissolution-rate constant for gypsum-water reaction at room temperature (10^{-7} mol/cm^{2}s) is near the equivalent parameter for quartz-water interaction at 300 °C (10^{-9} mol/cm^{2}s), so our gypsum experiments lasting 10^6 s may roughly model ~3 yr within quartzite systems at the hypocenters of large earthquakes on the San Andreas fault.

Could such lithification by chemical processes also be the origin of slip instability during crustal earthquakes (Reches, 1999)? This question is partly addressed in recent investigations of time-dependent changes of fault-zone properties. Analysis of shear-wave anisotropy of the 1995 Kobe earthquake rupture on the Nojima fault indicated that fault-parallel fractures (NE-SW) dominated the rupture zone for a period of about one year after the earthquake (Tadokoro et al., 1999). In later measurements, 33–45 months after the event, this set disappeared, and a new set (E-W) emerged (Tadokoro and Ando, 2000) oriented parallel to the regional fracture set. These changes are attributed to healing (Tadokoro and Ando, 2002). According to the present analysis, healing would occur as open fractures within the Nojima fault zone are gradually filled by chemical precipitates, and this has been observed in cores from Nojima fault boreholes (Moore et al., 2000). Other indicators that in situ chemical cementation could be strengthening a fault zone are the temporal variations of the seismic velocity of trapped waves in active fault zones. Two repeated surveys (1994 and 1996) of the Johnson Valley fault zone that slipped during the 1992 Landers earthquake revealed that P- and S-wave velocities increased by 0.5%–1.5% between the two surveys, suggesting a reduction of crack density (Li et al., 1998). Future measurements of similar phenomena would allow accurate evaluation of the time needed to fully regain fault-zone strength.

The hold-slide cycling on water-saturated fault gouge in our experiments is an appealing analog for earthquake-slip instability. Continued gouge lithification by time-dependent chemical processes during long interseismic periods would reform a fault zone into intact rock. The slip instability during subsequent rupture would then be best described as failure of a brittle, cohesive fault zone. The competition between rates of tectonic loading and rates of lithification could determine time to failure and earthquake recurrence (Reches, 1998).

ACKNOWLEDGMENTS

We thank J. Fineberg, S. Hickman, D. Lockner, A. Agnon, and B. Evans for valuable discussions. The comments of T. Tullis and C. Marone were very helpful. Financial support was provided by the U.S. Geological Survey National Earthquake Hazards Reduction Program, the Poromechanics Institute of the University of Oklahoma, and United States–Israel Binational Science Foundation grant 98/135.

REFERENCES CITED

Byerlee, J., Mjachkin, V., Summers, R., and Voevoda, O., 1978, Structures developed in fault gouge during stable sliding and stick-slip: Tectonophysics, v. 44, p. 161–171.

Dieterich, J.D., and Kilgore, B., 1994, Direct observation of frictional contacts; new insights for state-dependent properties: Pure and Applied Geophysics, v. 143, p. 283–302.

Jaeger, J.C., and Cook, N.G., 1979, Fundamentals of rock mechanics: London, Chapman and Hall, 515 p.

Karner, S.L., Marone, C., and Evans, B., 1997, Laboratory study of fault healing and lithification in simulated fault gouge under hydrothermal conditions: Tectonophysics, v. 277, p. 41–55.

Li, Y.G., Vidale, J.E., Aki, K., Fei, X., and Burdette, T.R., 1998, Evidence of shallow fault zone strengthening after the 1992 M7.5 Landers, California, earthquake: Science, v. 279, p. 217–219.

Logan, J.M., Dengo, C.A., Higgs, N.G., and Wang, Z.Z., 1992, Fabrics of experimental fault zones; their development and relationship to mechanical behavior, *in* Evans, B., and Wong, T.-F., eds., Fault mechanics and transport properties in rocks (the Brace volume): London, Academic Press, p. 33–67.

Mair, K., and Marone, C., 1999, Friction of simulated fault gouge for a wide range of velocities and normal stresses: Journal of Geophysical Research, v. 137, p. 28,899–28,914.

Marone, C., and Scholz, C.H., 1989, Particle-size distribution and microstructures within simulated fault gouge: Journal of Structural Geology, v. 11, p. 799–814.

Moore, D.E., Lockner, D.A., Ito, H., and Ikeda, R., 2000, Proceedings of the international workshop on the Nojima fault core and borehole data analysis: U.S. Geological Survey Open-File Report 00-129, p. 159–165.

Muhuri, S., 2002, Mechanisms and rates of strength recovery in laboratory faults [Ph.D. thesis]: Norman, University of Oklahoma, 184 p.

National Research Council, 2002, Living on an active earth: Perspectives on earthquake science: Washington, D.C., National Academy of Science, 43 p.

Olsen, M.P., Scholz, C.H., and Leger, A., 1998, Healing and sealing of a simulated fault gouge under hydrothermal conditions: Implications for fault healing: Journal of Geophysical Research, v. 103, p. 7421–7430.

Power, W.L., Tullis, T.E., and Weeks, J.D., 1988, Roughness and wear during brittle faulting: Journal of Geophysical Research, v. 93, p. 15,268–15,278.

Reches, Z., 1998, Earthquake nucleation as a brittle yielding process within a healed, intact fault zone: European Seismological Commission, XXVI General Assembly, Tel-Aviv, p. 77–82.

Reches, Z., 1999, Mechanisms of slip nucleation during earthquake: Earth and Planetary Science Letters, v. 170, p. 475–486.

Sleep, N.H., and Blanpied, M.L., 1992, Creep, compaction, and the weak rheology of major faults: Nature, v. 359, p. 687–690.

Tadokoro, K., and Ando, M., 2000, Evidence for rapid fault healing derived from temporal changes in S wave splitting [abs.]: Eos (Transactions, American Geophysical Union), v. 81, p. F1173.

Tadokoro, K., and Ando, M., 2002, Evidence for rapid fault healing at the Nojima fault, Japan, *in* Ogasawara, H., et al., eds., Seismogenic process monitoring: Rotterdam, A.A. Balkema, p. 201–220.

Tadokoro, K., Ando, M., and Umeda, Y., 1999, S wave splitting in the aftershock region of the 1995 Hyogo-ken Nanbu earthquake: Journal of Geophysical Research, v. 104, p. 981–991.

Manuscript received 17 February 2003
Revised manuscript received 9 June 2003
Manuscript accepted 12 June 2003

Printed in USA